

Effect of Silicon Addition on the Characteristics of Nitinol Shape Memory Alloy



Abdullah D. Assi^{1*}, Salman H. Omran², Moaz H. Ali³, Hussain Ali Hussain⁴, Ahmed A. Shandookh⁵

¹ Mechanical Engineering Department, College of Engineering, University of Baghdad, Baghdad 10071, Iraq

² Energy and Renewable Energies Tech. Center, University of Technology- Iraq, Baghdad 10066, Iraq

³ College of Engineering, University of Kerbala, Karbala 56001, Iraq

⁴ Advance Welding Solutions Company Ltd., Baghdad 10071, Iraq

⁵ Mechanical Engineering Department, University of Technology- Iraq, Baghdad 10071, Iraq

Corresponding Author Email: [Ahmed.A.Shandookh@uotechnology.edu.iq](mailto:Aхmed.A.Shandookh@uotechnology.edu.iq)

Copyright: ©2025 The authors. This article is published by IIETA and is licensed under the CC BY 4.0 license (<http://creativecommons.org/licenses/by/4.0/>).

<https://doi.org/10.18280/ijcmem.130111>

ABSTRACT

Received: 3 November 2024

Revised: 2 March 2025

Accepted: 13 March 2025

Available online: 31 March 2025

Keywords:

mechanical properties, nitinol, shape memory alloy, silicon

The effects of adding silicon to shape memory alloy (SMA) (Nitinol) were investigated in the current investigation. Most people think that silicon-based SMAs could be a cheaper alternative to NiTi SMA because they have good shape memory properties, good damping capacity, and other useful properties. The alloys were mechanically tested for Vickers microhardness, compression force, shape memory effect (strain recovery), density, and porosity to estimate the Si effect. Powder metallurgy was used to make the alloys. The base alloy (Nitinol) was prepared after sintering treatment at a temperature of 850°C for a period of 6hr. In addition, alloys were prepared from them to find out the effect of adding silicon. These alloys included the base alloy to which silicon was added in proportions of 0%, 3%, 6%, and 9% wt. of Si as their weight ratios. The results showed that increasing the percentage of silicon resulted in improved mechanical properties while 9.0 wt.% Si showed better shape memory properties.

1. INTRODUCTION

Recently, Shape Memory Alloys (SMA) have received significant attention in many commercial applications because of their specific and superior properties for remembering their original shape, (SMAs) are essentially different from other materials owing to pseudo elasticity (PE) and shape memory effect (SME) which are related to the particular way in which (phase transformation) occurs, wear and fatigue resistance, high power to weight ratio and biocompatibility. In the early 1960s, Buehler as well as his coworkers at the U.S. Naval Ordnance Laboratory (NOL) exposed a Shape Memory Effect (SME) for Ni and Ti Equi atomic alloy that may be considered an advance in the field of Shape Memory Materials (SMMs). This SMA was called Nitinol, where (NiTi) means Nickel and Titanium, while (NOL) means Naval Ordnance Laboratory.

Intensive studies have been conducted since then to elucidate the mechanisms of its basic behavior [1, 2]. NiTi-based, Fe-based, and Cu-based SMAs are the three main types of shape-memory alloys that are used. Most of the time, (NiTi-based) alloys are used because of their Super elasticity (SE) and Shape Memory Effect (SME) [3, 4]. Fe-based and Cu-based SMAs, like (CuZnAl), (CuAlNi), and (FeMnSi), are cheap and available commercially, but their use is limited because they don't have good thermal cycle properties and have low yield stresses [5, 6]. Metallic alloys (NiTi) have a Shape Memory Effect (SME) property, which makes them an interesting material. NiTi SMA is used widely in a variety of

applications, such as robotics, telecommunication, medicine, and electronics. Nitinol alloy is the most excellent material for binary alloys. But SMAs have many disadvantages which make them unappreciated in many applications. The possible solution is to modify these alloys' amalgamation, or else the chemical composition of the manufacturing method [7, 8].

Depending on the temperature, Nitinol can exist in the martensite phase (B19), the austenite phase (B2), or a mixture of both phases. SMA often transforms the austenite phase, which occurs at high temperatures, and the martensite phase at low temperatures. SMA phase changes can be influenced by many variables, including processing methods, nickel concentration variations, heat cycling, combined thermomechanical treatment, and ternary alloying components [9, 10]. Zeng et al. [11] reported that superelastic and SME have a high amount of Ni. The bending and actuation of a device are obtained by resistivity heat, which activates the shape memory effect of variant laser-processed points. The findings of this study demonstrated that electrical-thermo-mechanical processing of a laser-processed area may be done at a variable current depending on the temperature. Shelyakov et al. [12] reported the effect of cooling rate on the thickness of non-crystalline Ti-Ni-Cu two-way SMA at about 40µm of thickness, and the separating of crystalline and non-crystalline phases into the layers was prepared using a melting spinning route. The findings of this study show that, concerning the mechanical 3D manipulator, the microgripper can move with an accuracy of around 2 µm. Omran et al. [13] studied the

effect of adding elements Sn, Cu, and Co on the properties of the SMA by casting method (VIM furnace). The thermal treatment of the specimens prepared for 15 minutes was carried out at (865°C) in normal conditions, after which it was cooled with ice water. The tests of Vickers microhardness for (NiTi) SMA showed an improvement through adding Cu and Co before and after thermal treatment. Ahmed Adnan [14] looks at what happens when Sn is added to a shape-memory alloy made of Cu-14% and Al- 4.5% Ni. There were three different amounts of Sn addition 0.3%, 1%, and 3%. Compression tests and microhardness tests were used to determine the mechanical properties of the alloys. Mechanical properties showed the best results, while the 3% Sn showed better Shape Memory Properties that were close to superelastic.

Shihab et al. [15] studied nanoparticles of Ag (which are insoluble in the Ni-Ti matrix), which are added to the Ni-Ti alloy using powder technology to form a Ni-Ti-Ag alloy. Nanoparticles of the element Ag are added at concentrations of 3, 5, 7, and 10 wt.% to form four alloy specimens with distinct compositions. The findings of this study demonstrated that Nano-Ag injected at 7 and 10 wt.% was distributed uniformly throughout the Ni-Ti matrix and that Ag marginally lowered hardness and increased the wear rate. Salman et al. [16] studied samples of Ni-Ti shape-memory alloy with different amounts of Ag nanoparticles are made and their density, porosity, and ability to conduct electricity are studied. Utilizing the powder technique, the specimens are created. There were no noticeable differences in the distribution of the Ag nanoparticles in the Ni-Ti matrix, and the austenite and martensite phases developed as a result of these tests. A strong SME was also demonstrated by the researchers 89.9% for the 10 wt.% percentage of Ag nanoparticles). Stachowiak and Kurzawa [17] studied the combination of experiment and the computational of designing two different springs, composed of steel and SMA. The results of this work show that the mathematical model for stroke and temperature of SMA spring has been successfully applied. Hattori et al. [18] studied the impact of the Pd element on the shape memory properties of NiTi SMA. The findings of this study revealed that the martensitic transition temperature reduced as Ti content increased or decreased (with constant stress). During the thermal cycling Pd and Ti₂Pd phase, the shape memory properties, stability of dimensions, and large work output are improved under constant stress.

Copaci et al. [19] reported the comparison between conventional actuators and actuators based on the SMAs. These actuators are widely used in medical applications, automation, and robots. During the first stage, operating, its temperature is obtained from the Joule effect and then the electrical energy will transform to mechanical work. During the second stage, thermal energy will transform into mechanical work. The results of this work show that the best model depends on the two stages mentioned above. Abdullah et al. [20] aimed to enhance the performance of SMA-based soft grippers for diverse applications. Soft robotics uses flexible materials instead of rigid ones. This study explores using SMA wires as artificial muscles embedded in silicone for soft grippers. Simulation and experimental studies were conducted on various SMA wire configurations to assess their performance regarding tip displacement, tip force, and bending angle.

SMAs possess unique properties like shape memory effect (SME) and pseudoelasticity (PE), making them suitable for

various applications. However, SMAs face limitations such as wear and fatigue resistance, high power-to-weight ratio, and biocompatibility issues. The primary SMA types include NiTi-based, Fe-based, and Cu-based alloys. NiTi-based alloys are preferred due to their superelasticity and SME, while Fe-based and Cu-based alloys are cheaper but have lower thermal cycle properties and yield stress. Modifying the alloy composition or manufacturing methods can address these issues. Various factors, such as processing methods and nickel concentration variations, can influence the transformation between the martensite (low temperature) and austenite (high temperature) phases in SMAs.

Recent studies focus on improving the mechanical properties, shape memory properties, and superelasticity of SMAs through various treatments and alloy compositions. Applications range from robotics, telecommunications, medicine to electronics and more. Hence, this paper uses powder technology to add three different percentages of Si to study the effects of Si addition on the mechanical and shape memory properties of Nitinol SMA, investigate density, porosity, compression force, shape effect (strain recovery), and micro-hardness, and estimate the Si effect.

After presenting the applications of this alloy, the experimental procedures are carried out in terms of preliminary examinations of chemical analysis and mechanical properties, the mold is manufactured, and the ingot is produced from powder to prepare samples and conduct other mechanical and physical examinations and tests.

2. APPLICATIONS OF NITINOL SMA

The main applications of Nitinol SMA are aerospace, actuators, shock absorbers, pipe coupling, automotive applications, human devices, window frames, eyeglasses, antennae of cellular phones, and SMA springs in water mixers and other applications thereof [21].

2.1 Biomedical applications

For many decades, there has been an effort between engineering, scientific, and medical to manufacture materials that can be used to prevent a certain disease. For example, in implants, most of these materials proved hazardous to human health.

- a. Orthodontics
- b. Neurosurgery
- c. Ophthalmology

2.2 Industrial applications

Owing to their novel properties, SMA can be used in different industrial applications. Especially, applications in robots, aeronautics, and tube coupling.

3. EXPERIMENTAL WORK

3.1 Description of materials

Ni-Ti-Si particle powders were used to manufacture SMA. Tables 1 and 2 show the properties of the powders used in this thesis. The test specimens are produced using the powder metallurgy method (PM) from Ni, Ti, and Si, which consists

of mixing, blending, compacting, and sintering processes. SMAs are created with high-quality titanium metal with 99.84 wt.%, nickel with 99.84 wt.%, and silicon with 99.85 wt.% which have been utilized as an additional element at concentrations of 3, 6, and 9 wt.% of Si.

Table 1. Chemical composition and physical properties as metal matrix [22]

Metal Matrix	Ni	Ti
% Fe	0.05	0.05
% S	0.01	0.02
% C	0.05	0.05
% O	0.05	0.04
Density (g/cm ³)	8.908	4.506
Particle size (μm)	40	50
Mesh	58	58
Purity	99.84	99.84

Nitinol is known for its shape memory effect along with good kink resistance, thermomechanical properties of superplasticity, and portability [23, 24]. Ni-Ti SMA alloy may contain two phases for the final products as shown in Figure 1.

Table 2. Chemical and physical properties of si particles metal [22]

Material	Practical	Purity	Density (g/cm ³)
Si powder	63	99.85	2.33

Table 3. Different weight percentages of Ni, Ti, and Si

Specimens	Ni (wt.%)	Ti (wt.%)	Si (wt.%)
Base	50	50	0
S1	47	50	3
S2	44	50	6
S3	41	50	9

Table 4. Physical and mechanical properties of nitinol SMA [18]

Properties of Nitinol SMA	Values	Unit
Modulus of Elasticity	75 (austenite) 40 (martensite)	GPa
Yield Strength	195-690 (austenite) 70-140 (martensite)	MPa
Ultimate Tensile Strength	895-1000	MPa
Poisson Ratio	0.30	-
Shear Modulus	28.8	GPa
Shape Memory Strain	8.5	%
Density	6.45	g/cm ³
Melting Temperature	1310	°C
Electrical Resistivity (austenite)	100	μΩ.cm
Electrical Resistivity	80	μΩ.cm
Thermal Conductivity (austenite)	18	W/cm. °C
Thermal Conductivity (martensite)	8.5	W/cm. °C
Transformation Temperature	-200-100	°C
Transformation Hysteresis	30-50	°C

The varied weight percentages of the matrix element (Nitinol) and silicon element as additive materials are displayed in Table 3.

Table 4 shows the Characteristics of Nitinol SMA which are extremely dependent on the composition and phase of this alloy. Equi atomic Nitinol contains 50 wt.% Ni and 50 wt.% Ti; this alloy is considered an intermetallic compound.

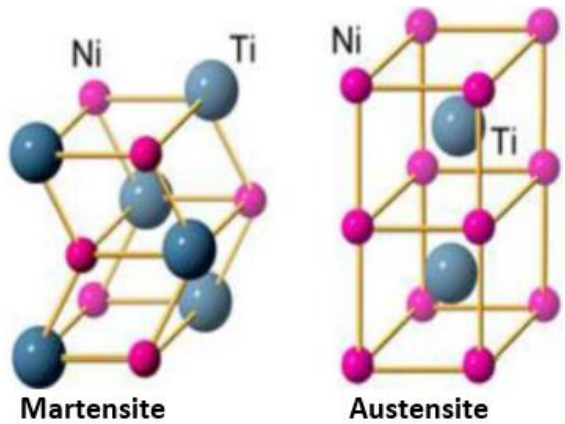


Figure 1. A right austenite (B2) and left martensitic (B19) [23]

3.2 Powder metallurgy method

In this method, various techniques can be used to produce NiTi alloy by using Ni and Ti powders. This method involves three stages as follows: the first stage is the mixing process to prepare a uniform and good distribution of starting powders in a proper concentration. The second stage is a compacting process using high pressure to obtain a green compact. In this process, the products are prepared for handling to afford the applied loads. The third stage is a sintering process to obtain the required density, this process was done using a sintering furnace at a temperature below the melting point to promote the diffusion of each particle to take place. Increasing the sintering temperature leads to form necks with less surface energy compared with other spherical particles. In this stage, the pores are almost uniform, and Kirkendall's porosity may be greater [22]. Commonly, the main advantage of this method involves a good homogeneous composition of the product compared with the vacuum remitting method (VAR), and the products with high porosity, which restricts them to use for biomedical applications.

3.3 Compacting process



Figure 2. Sketch of single-action tool steel mold [24]

The cold compacting process was carried out by the Tinus Olsen test at a pressure of 500 and 700 MPa using uniaxial force for the tool steel mold [23]. The tool steel mold consists

of an upper punch and a lower punch with a diameter of about 12 mm. The mold was filled with the powder mixture and then pressed in the uniaxial direction. Holding the time for pressing 6 min to obtain the desired dimensions of the compacted specimens. After that, the specimens were ejected by removing the lower punch and pressing the upper punch into the mold cavity. Figure 2 shows the steps of the compacting process to obtain the green [24].

3.4 The manufacturing process

The manufacturing process of SMA (NiTi) is very important and has an impact on the properties of the produced alloys as well as on homogeneity, uniform distribution, and microstructure [25]. The manufacturing process is generally divided into the casting method and powder method, followed by mechanical processes such as cold working, hot working, annealing, and surface treatment. The first way to produce smart alloys is the powder method, which involves several techniques [26]. The materials used should be pure materials with high cleanliness, as far as possible from the presence of non-metallic materials, and non-metallic elements can seriously affect the homogeneity and unity of the alloy, creating uneven formation distribution and changing fundamental properties of the material [27].

Studying the influence of Si % on the physical and mechanical characteristics of SMA was done using powder metallurgy. The basic combination (Nitinol) is made with a ball mill for six hours, while other specimens are prepared with a sand mill by 3, 6, and 9 wt.% Si. Following mixing, two different types of powder specimens were created in the same die, each measuring 15 mm in diameter and 6 mm in thickness, 15 mm in diameter, and 20 mm in length. The specimens were pressed at 500 and 700 MPa in a computerized uniaxial press with a 100KN load capacity, 1mm/minute displacement rate, and 5-minute holding time. The machine also had a load-holding period of 5 minutes. Sintering of the specimens' compacts took place in a vacuum tube furnace at this stage of the procedure. The sintering process begins by heating the material to 850°C for six hours. After that, the sintered specimen is allowed to cool in the furnace. Throughout the sintering process, a constant heating rate of 20°C/min is applied [28].

3.5 Specimen preparation

After being subjected to sintering and quenching treatment, the specimens are given grinding treatment with paper grits of 180, 400, 800, 1000, and 2000, then they are polished with alumina at room temperature. All specimens were then dried using an electric dryer and washed in distilled water. For imaging of specimen surfaces, a light optical microscope of the Union ME-3154 type is utilized [29].

3.6 Mechanical tests

Vickers microhardness (VMH) test was used to estimate the hardness of the sintered SMA [30]. Before testing, the sintered specimens were ground by emery papers with grit sizes 1000 μm and 2000 μm and then polished by polished cloth with alumina. After that, the specimens were tested by the Vickers hardness apparatus type TH-715 for 25 seconds and 20 kg. At least five readings for each specimen were taken, and then calculated the average of the indenter diameter [31]. Using a

uniaxial compression apparatus, a shape memory effect (SME) test was conducted to examine the SME and the percentage of maximum strain returned after heating. This was done by figuring out the length of the specimens before they were compressed (L_0), then compressing them to 6 percent strain (the maximum strain back for silicon base), and letting them go. After that, they were measured again to find out how long they were after being compressed (L_1). Using the following equation, the shape memory effect will be estimated by measuring these lengths [32]:

$$\text{Strain_Recovery(shape_effect)} = \frac{L_0 - L_2}{L_0 - L_1} \times 100\% \quad (1)$$

where,

L_0 : normal specimen length.

L_1 : The length of the specimen after 0.06 % of its length was compressed.

L_2 : length of the sample after 6 minutes at 200°C.

Using Archimedes' rule and a Hock balance device, the porosity of a sample was determined by weighing it in air, placing it in a basket filled with distilled water, soaking it for 20 hours in distilled water, and then weighing it after drying. The apparent porosity and bulk density were calculated using Eqs. (2)-(3), respectively [33].

$$\text{pparent_Porosity} = \frac{w_s - w_d}{w_s - w_n} \times 100\% \quad (2)$$

$$\text{Bulk_Density} = \frac{w_d}{w_s - w_n} \times \rho_d \quad (3)$$

where w_d is the dried specimen's weight, w_s is specimen weight in the basket, w_n weight of the sample after 20 hours of storage in distilled water and ρ_d is the density of distilled water [34].

4. RESULTS AND DISCUSSION

4.1 Microstructures of the shape memory alloy

After comparing Figures 3(a) and 3(b), it is evident that the substitution of nickel with silicon alters the microstructure morphology of Ni-Ti SMA at room temperature, about 25°C. The lack of martensite variations in SMA, Ni-Ti, and Ni-Ti-Si may be confirmed. The start and end martensite transition temperatures (M_S and M_F) in both SMAs are below room temperature. For alloys with compositions ranging from 0.5 to 9 wt.%. There are no published studies on changes in microstructural morphology.

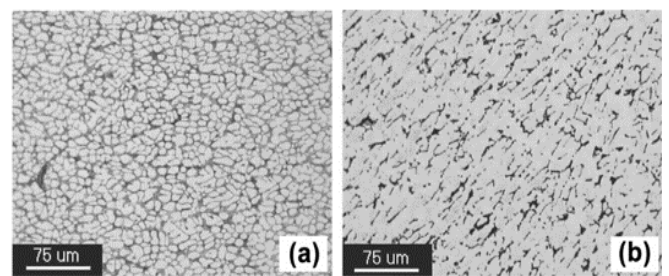


Figure 3. Microstructures of the investigated SMA. (a) Ni-Ti and (b) Ni-Ti-Si

4.2 Effect of silicon addition on the shape memory effect

For 500 MPa and 700 MPa compacting pressures, the shape memory effect (SME) is depicted in Figure 4 as a function of silicon content. The retaining length recovery percentage is shown as a percentage. The shape memory effect (SME) varied between 96% and 97% for 500 MPa and between 95.5% and 97.5% for 700 MPa, indicating that this element produced an excellent martensitic structure, which was subsequently changed into a good austenite phase.

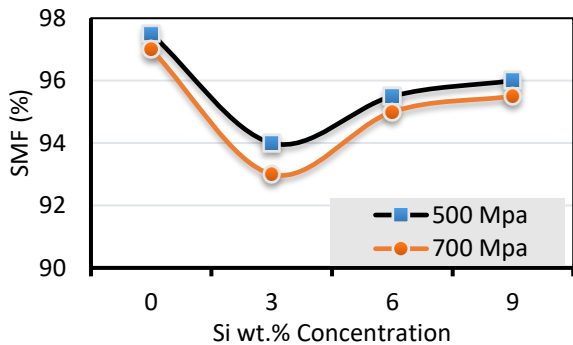


Figure 4. Shape memory effect (SME) as a function of Si content for 500 and 700 MPa

4.3 Effect of Si addition on the Vickers micro hardness

The Vickers microhardness (VMH) test was performed on each specimen before and after adding Si at various weight percentages of 0, 3, 6, and 9 of Si. As shown in Figure 5, the findings of this experiment show that as the weight% of Si grew, hardness decreased. When the compacting pressure was 500MPa and the amount of silicon went from 0 to 9 wt. The reduction was about 38%. When the compacting pressure was 700 MPa, the reduction was about 34%. This is because the shape memory effect (SME) is getting stronger at about 97.5% for 500 Mpa and 97.5% for 500 Mpa, and the defects in the resulting SMA, like micro-cracks and porosity, are getting smaller.

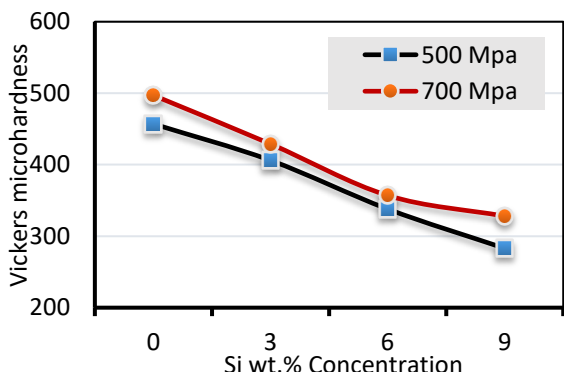


Figure 5. Vickers microhardness as a function of silicon content at 500 and 700 MPa compacting pressure

These flaws depend a lot on the pressure used to pack the material down and the temperature at which it is sintered. They also have a direct effect on the hardness values. Ni-Ti-Si alloys have a lower hardness than their NiTi alloy counterparts, which may be explained by the form of the microstructure. Also, other physical things, like the binding energy and

wettability between Si particles and Ni-Ti grains, may affect the hardness values. Because silicon addition makes the material more brittle, the decreased hardness in Ni-Ti-Si is believed to be because it reduces the stress required to induce or realign martensite variations.

4.4 Effect of Si addition on the compression force

Figure 6 depicts the silicon addition at 500MPa and 700MPa compacting pressure. It shows an increase in applied force with (0, 3, 6, and 9 wt. % Si) addition. Figure 6 shows Compression force as a function of silicon content.

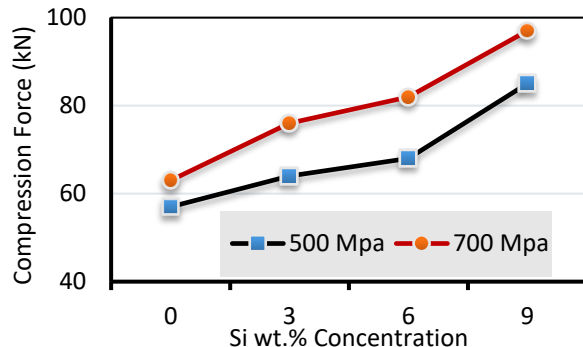


Figure 6. Compression force as a function of silicon content for 500 and 700 MPa

For example, it can be seen from the compression force data in Figure 6 that increasing the compacting pressure from 500 MPa to 700 MPa and the silicon percent to 9 wt.% enhances the master alloy's compression strength. Higher compressive pressure and the addition of silicon may be to blame for this behavior. This is because silicon makes the material more brittle, which improves its compression force and reduces stress concentration areas, such as pores and microcracks, which may cause the alloy to fail prematurely.

4.5 Effect of Si addition on the density and porosity

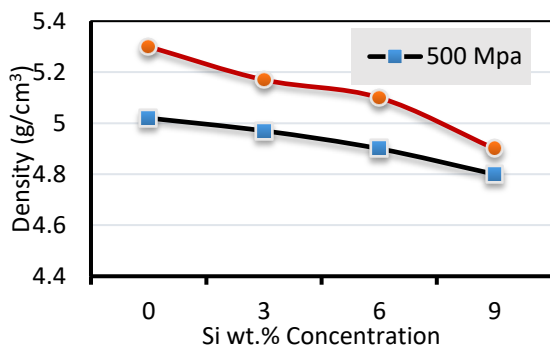


Figure 7. The density as a function of the concentration of silicon for 500 and 700 MPa compacting pressures

Figure 7 depicts the influence of silicon content on master alloy density. As shown in the Figure, an increase in silicon percentage from 0, 3, 6, and 9 wt.% Si decreases the density by a few percentage points up to 4.38 percent at a compacting pressure of 500 Mpa and 7.54% at a compacting pressure of 700 MPa, indicating that density increases with decreasing silicon content. To enhance the powder mass's density, you must increase the amount of pressure used to compact it. When

a single-level cylindrical compact is punched from one direction, the compressive stress delivered to the top punch is not equally distributed in direction and amplitude. It's because of this friction that there are differences in density throughout the pressing path. We may lessen this friction by cleaning the dies with acetone after each compaction stage.

4.6 Effect of silicon addition on the porosity of master alloy

Figure 8 shows the relationship between porosity and silicon content at 500 MPa and 700 MPa. Increasing the compacting pressure makes the powder mass denser because the total number of holes in the mass goes down. When the compacting pressure was 500 MPa, the porosity went up by 21.20 percent. When the compacting pressure was 700 MPa, the porosity went up by 24.05%.

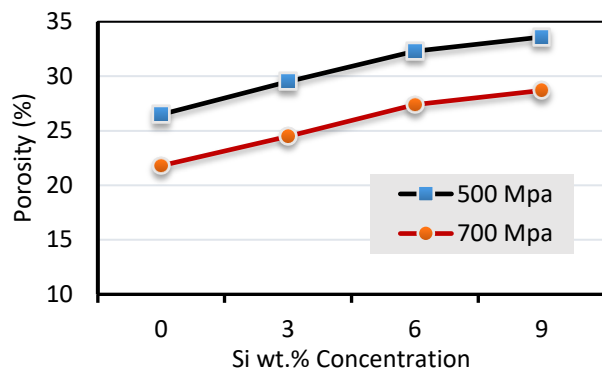


Figure 8. The porosity as a function of silicon concentration at 500 and 700 MPa compacting pressures

As shown in Figure 9, the density after sintering changes with silicon content at compacting pressures of 500 and 700 MPa. After sintering, the density is greater than the density at all compacting pressure levels. This increase is most likely the result of the initial pores contracting during the sintering process. The increase in density was around 7.33 percent at a compacting pressure of 500 MPa and 7.55 percent at a pressure of 700 MPa. With increased sintering time, the initial pores decrease in size.

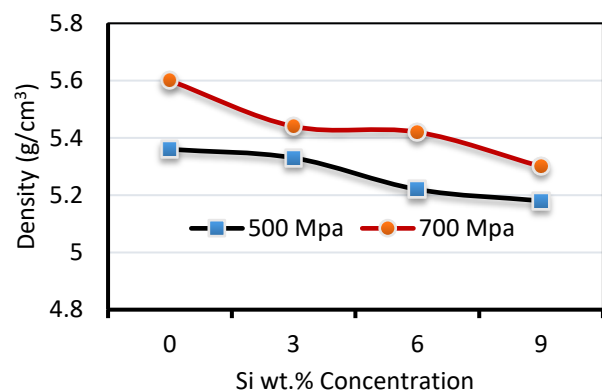


Figure 9. The density after sintered as a function of silicon concentration for 500 and 700 MPa compacting pressures

As can be seen in Figure 10, sintering for six hours at 850°C results in a significant drop in density for all of the compositions tested. After sintering, a decrease in density is

strongly associated with an increase in porosity. It is because silicon atom diffusion in titanium is several times more than nickel atom diffusion in titanium that this rise occurs. Furthermore, compared to silicon or nickel, titanium has a greater silicon-to-nickel or titanium-to-silicon atom diffusion ratio. Since silicon and nickel initially diffuse into an alloy, titanium particles are essential as building blocks. Pore size increases as a result of this process. Using this method, smaller pores can be made where the titanium particles meet the silicon/nickel. As the sintering temperature goes up, the diffusion gets faster, and the pores get bigger on average.

As can be seen in Figure 10, sintering for six hours at 850°C results in a significant drop in density for all of the compositions tested. After sintering, a decrease in density is strongly associated with an increase in porosity. It is because silicon atom diffusion in titanium is several times more than nickel atom diffusion in titanium that this rise occurs. Furthermore, compared to silicon or nickel, titanium has a greater silicon-to-nickel or titanium-to-silicon atom diffusion ratio. Since silicon and nickel initially diffuse into an alloy, titanium particles are essential as building blocks. Pore size increases as a result of this process. Using this method, smaller pores can be made where the titanium particles meet the silicon/nickel. As the sintering temperature goes up, the diffusion gets faster, and the pores get bigger on average.

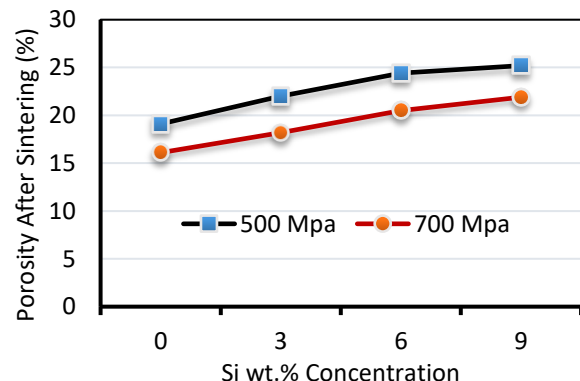


Figure 10. The Porosity after sintering as a function of silicon content at 500 and 700 MPa compaction pressures

5. CONCLUSION

The conclusions obtained from the experimental procedures were:

- Preparing SMA Ni-Ti-Si by using the powder technology (PT) method with different percentages of 0, 3, 6, and 9 wt.% of Si. Powder compacting requires a pressure force of 700 MPa. This is found by using pressure forces of 500 MPa and 700 MPa to compact samples.

- Scanning Electron Microscopy (SEM) images revealed a homogenous distribution of Si in the Ni-Ti matrix. The results of the shape memory effect (SEM) showed that the best value of the shape memory effect was 97.5% for 500 MPa, and 97 % for 700 MPa at the highest percentage of 9 wt. % Si.

- VMH values decreased with increasing the percentage of Si, Si reduces the SFE in these alloys enhancing the nucleation of stress-induced martensite and consequently the amount of shape recovery.

- Increasing silicon content decreases hardness whereas increasing silicon content increases compression force; also,

700 MPa of compacting pressure produces a greater compression force than 500 MPa.

The density increased with increasing the amount of Si, while the porosity decreased with increasing the amount of Si. Also, the volumetric percentage of porosity decreases as the compacting stress increases.

The shape memory effect test reveals that all silicon content levels of 3, 6, and 9 wt. % have an excellent martensitic structure, which is later changed into a good austenite phase.

For further studies in the same line of the paper, it is recommended to look into the temperature effect on the existence of Nitinol in the martensite phase (B19), the austenite phase (B2), and the R-phase. Also, Smart alloys are the powder method and involve several techniques. Other techniques are recommended to be investigated.

ACKNOWLEDGMENT

The authors would like to thank the Universities of (Baghdad, University of Technology, and Kerbala) for supporting this hard research work.

REFERENCES

- [1] Huang, W.M., Ding, Z., Wang, C.C., Wei, J., Zhao, Y., Purnawali, H. (2010). Shape memory materials. *Materials Today*, 13(7-8): 54-61.
- [2] Tatar, C., Kurt, M. (2020). Phase transformation temperatures and physical characteristics of NiTiCo shape memory alloys produced by arc melting method. *The European Physical Journal Plus*, 135(9): 765. <https://doi.org/10.1140/epjp/s13360-020-00737-6>
- [3] Petrini, L., Migliavacca, F. (2011). Biomedical applications of shape memory alloys. *Journal of Metallurgy*, 2011(1): 501483. <https://doi.org/10.1155/2011/501483>
- [4] Aljebouri, A.A., Mohammed, S.H., Mohammed, M.A. (2020). Effect of Sn addition on phase transformation behavior of equiatomic Ni-Ti shape memory alloy. *Baghdad Science Journal*, 17(3): 46. [https://doi.org/10.21123/bsj.2020.17.3\(Suppl.\).0961](https://doi.org/10.21123/bsj.2020.17.3(Suppl.).0961)
- [5] Maruyama, T., Kubo, H. (2011). Ferrous (Fe-based) shape memory alloys (SMAs): Properties, processing and applications. In *Shape Memory and Superelastic Alloys*, Woodhead Publishing, pp. 141-159. <https://doi.org/10.1533/9780857092625.2.141>
- [6] Yamauchi, K. (2011). Development and commercialization of titanium-nickel (Ti-Ni) and copper (Cu)-based shape memory alloys (SMAs). In *Shape Memory and Superelastic Alloys*, Woodhead Publishing, pp. 43-52. <https://doi.org/10.1533/9780857092625.1.43>
- [7] Szurma Kocich, R., Szurman, I., Kursa, M. (2013). The methods of preparation of Ti-Ni-X alloys and their forming. *Shape Memory Alloys-Processing, Characterization and Applications*, pp. 28-35. <https://doi.org/10.5772/50067>
- [8] Abdulrusool, A., Mosa, S.J. (2016). The effective of pressure and sintering temperature for hardness characteristics of shape memory alloy by using Taguchi technique. *Journal of Engineering*, 22(1): 159-171. <https://doi.org/10.31026/j.eng.2016.01.10>
- [9] Grigorie, T.L., Popov, A.V., Botez, R.M., Mamou, M., Mébarki, Y. (2012). On-off and proportional-integral controller for a morphing wing. Part 1: Actuation mechanism and control design. *Proceedings of the Institution of Mechanical Engineers, Part G: Journal of Aerospace Engineering*, 226(2): 131-145. <https://doi.org/10.1177/0954410011408226>
- [10] Alfay, R.Z., Takhakh, A.M., Ali, A.R. K.A. (2014). Effect of Nb Addition on hardness and wear resist of Cu-Al-Ni shape memory alloy fabricated by powder metallurgy. *Journal of Engineering*, 20(1): 42-49. <https://doi.org/10.31026/j.eng.2014.01.04>
- [11] Zeng, Z., Oliveira, J.P., Ao, S., Zhang, W., Cui, J., Yan, S., Peng, B. (2020). Fabrication and characterization of a novel bionic manipulator using a laser processed NiTi shape memory alloy. *Optics & Laser Technology*, 122, 105876. <https://doi.org/10.1016/j.optlastec.2019.105876>
- [12] Shelyakov, A., Sitnikov, N., Borodako, K., Koledov, V., Khabibullina, I., von Gratowski, S. (2020). Design of microgrippers based on amorphous-crystalline TiNiCu alloy with two-way shape memory. *Journal of Micro-Bio Robotics*, 16: 43-51. <https://doi.org/10.1016/j.mser.2007.03.001>
- [13] Omran, S.H., Assi, A.D., Ali, M.H., Shandook, Ahmed A., Abbud, L.H., Abdul Wahhab, H.A. (2023). Fatigue and hardness behavior of Al-2Cu-2mg Alloy due to titanium dioxide and silicon carbide nano-additives. *Journal of Engineering Science and Technology*, 18: 240-254. https://jestec.taylors.edu.my/Special%20Issue%20on%20ICSSD2023/ICSSD2023_17.pdf.
- [14] Ahmed Adnan, R.S. (2020). Effect of Tin Addition on Shape memory effect and mechanical properties of Cu-Al-Ni shape memory alloy. *Engineering and Technology Journal*, 38(8A): 1178-1186. <https://doi.org/10.30684/etj.v38i8A.440>
- [15] Shihab, S.A., Salman, K.D., Saud, L.J. (2020). Studying wear behavior of Ni-Ti-Ag shape memory alloy synthesized by P/T. T, 38(6): 846-853. <https://doi.org/10.30684/etj.v38i6A.463>
- [16] Salman, K.D., Saud, L.J., Shihab, S.A. (2020). Characterization of Ni-Ti-Ag shape memory Alloy. In *IOP Conference Series: Materials Science and Engineering*, pp. 012053. <https://doi.org/10.1088/1757-899X/765/1/012053>
- [17] Stachowiak, D., Kurzawa, M. (2019). A computational and experimental study of shape memory alloy spring actuator. *Prz. Elektrotechniczny*, 95: 29-32. <https://doi.org/10.15199/48.2019.07.07>
- [18] Hattori, Y., Taguchi, T., Kim, H.Y., Miyazaki, S. (2019). Effect of stoichiometry on shape memory properties and functional stability of Ti-Ni-Pd alloys. *Materials*, 12(5): 798. <https://doi.org/10.3390/ma12050798>
- [19] Copaci, D., Moreno, L., Blanco, D. (2019). Two-stage shape memory alloy identification based on the Hammerstein-wiener model. *Frontiers in Robotics and AI*, 6: 83. <https://doi.org/10.3389/frobt.2019.00083>
- [20] Abdullah, M.D.F., Wahid, A.N., Muthalif, A.G. (2023). Development of shape memory alloy (SMA) based artificial muscle for application in soft gripper. *Journal of*

- Engineering Science and Technology, 18(3): 1413-1426.
URL: JESTEC
- [21] Karamichailidou, S.X.D. (2016). The Unique Properties, Manufacturing Processes and Applications of Near Equatomic Ni-Ti Alloys, Ph. D. Thesis. <https://api.semanticscholar.org/CorpusID:143428237>.
- [22] Material Property Data. <https://www.matweb.com/>.
- [23] Groover, M.P. (2019). Fundamentals of modern manufacturing materials.
- [24] Assi, A.D., Abdulhadi, H.A., Omran, S.H. (2020). Effect of adding SiC and TiO₂ nanoparticles to AA6061 by stir casting technique on the mechanical properties of composites. Journal of Mechanical Engineering Research and Developments, 43(6): 167-183
- [25] Astm D570 – 98 (2018). Standard Test Method for Water Absorption., Developed by Subcommittee: D20.50, Book of Standards Volume, 08.01.2018. <https://doi.org/10.1520/D0570-98R18>
- [26] Li, P., Jia, Y., Wang, Y., Li, Q., Meng, F., He, Z. (2019). Effect of Fe addition on microstructure and mechanical properties of as-cast Ti49Ni51 alloy. Materials, 12(19): 3114. <https://doi.org/10.3390/ma12193114>
- [27] Andrade, C.A., Soares, F.D.A.D.S., Nobrega, G.T.V., Hilário, J. C., Santos, L. (2020). Characterization techniques of a shape memory nickel titanium alloy. Proceedings—Open Access Journal, Proceedings, 38(1): 15. <https://doi.org/10.3390/proceedings2019038015>
- [28] Sharma, P. (2018). NiTi shape memory alloy: Physical and tribological characterization. Journal of the Mechanical Behavior of Materials, 27(1-2): 20180009. <https://doi.org/10.1515/jmbm-2018-0009>
- [29] Naresh, C., Bose, P.S.C., Rao, C.S.P. (2016). Shape memory alloys: A state of art review. IOP Conference Series: Materials Science and Engineering, 149(1): 012054. <https://doi.org/10.1088/1757-899X/149/1/012054>
- [30] Fayad, M.A., Abed, A.M., Omran, S.H., Jaber, A.A., Radhi, A.A., Dhabhad, H.A., Chaichan, M.T., Yusaf, T. (2022). Influence of renewable fuels and nanoparticles additives on engine performance and soot nanoparticles characteristics. International Journal of Renewable Energy Development, 11(4): 1068-1077. <https://doi.org/10.14710/ijred.2022.45294>
- [31] Hassan, A.K., Abaas, A.A.A.N., Omran, S.H., Habeeb, L.J. (2020). Natural convection in eccentric annuli packed with spheres. Journal of Mechanical Engineering Research and Developments, 43(6): 418-439.
- [32] Omran, S.H., Shandook, A.A., Ali, M.H., Wahhab, H.A.A. (2023). Evaluation of electroplating effects on Mechanical Properties and Fatigue of AA7075-T6 alloy. Journal of Engineering Science and Technology, 18: 225-239.
- [33] Dhayea Assi, A., Thamer Abdulwahid, Z., Hussein Omran, S. (2023). The effect of heat treatment for alloys (Aluminum-Copper) on some mechanical properties. Solid State Phenomena, 345: 13-22. <https://doi.org/10.4028/p-p5DpGy>
- [34] Dhayea Assi, A., Thamer Abdulwahid, Z., Hussein Omran, S. (2023). The effect addition of (Silicon and Silver) and heat treatments to the alloy properties (Copper-Nickel-Tin). Solid State Phenomena, 345: 3-11. <https://doi.org/10.4028/p-g86KoE>

NOMENCLATURE

VIM	Vacuum Induction Melting
PE	Pseudoelasticity
NOL	Naval Ordnance Laboratory
SE	Super Elasticity
VAR	Vacuum Remitting Method

Subscripts

<i>Pd</i>	Density of Distilled Water
<i>w_d</i>	Dried Specimen's Weight,
<i>w_s</i>	Specimen Weight in the Basket
<i>w_n</i>	Weight of the sample after 20 hours of storage in distilled water
<i>M_S</i>	Martensite Transition Temperatures Start
<i>M_F</i>	Martensite Transition Temperatures Finished